Hypochlorous Acid-Mediated Protein Oxidation: How Important Are Chloramine Transfer Reactions and Protein Tertiary Structure?[†]

David I. Pattison,* Clare L. Hawkins, and Michael J. Davies

The Heart Research Institute, 114 Pyrmont Bridge Road, Camperdown, Sydney, New South Wales 2050, Australia

Received May 2, 2007; Revised Manuscript Received June 18, 2007

ABSTRACT: Hypochlorous acid (HOCl) is a powerful oxidant generated from H_2O_2 and Cl^- by the heme enzyme myeloperoxidase, which is released from activated leukocytes. HOCl possesses potent antibacterial properties, but excessive production can lead to host tissue damage that occurs in numerous human pathologies. As proteins and amino acids are highly abundant in vivo and react rapidly with HOCl, they are likely to be major targets for HOCl. In this study, two small globular proteins, lysozyme and insulin, have been oxidized with increasing excesses of HOCl to determine whether the pattern of HOCl-mediated amino acid consumption is consistent with reported kinetic data for isolated amino acids and model compounds. Identical experiments have been carried out with mixtures of *N*-acetyl amino acids (to prevent reaction at the α-amino groups) that mimic the protein composition to examine the role of protein structure on reactivity. The results indicate that tertiary structure facilitates secondary chlorine transfer reactions of chloramines formed on His and Lys side chains. In light of these data, second-order rate constants for reactions of Lys side chain and Gly chloramines with Trp side chains and disulfide bonds have been determined, together with those for further oxidation of Met sulfoxide by HOCl and His side chain chloramines. Computational kinetic models incorporating these additional rate constants closely predict the experimentally observed amino acid consumption. These studies provide insight into the roles of chloramine formation and three-dimensional structure on the reactions of HOCl with isolated proteins and demonstrate that kinetic models can predict the outcome of HOCl-mediated protein oxidation.

Hypochlorous acid (HOCl)[1] is a strong oxidant that has potent antibacterial properties and is produced in vivo by activated leukocytes as part of the mammalian immune defense system (*1*, *2*). Upon activation, leukocytes undergo a respiratory burst to produce superoxide via an NADPH oxidase enzyme system (*3*); the superoxide radicals rapidly dismutate to generate H_2O_2. Simultaneously, activated leukocytes release inflammatory mediators including cytokines and chemokines, together with a range of enzymes that can inactivate invading pathogens, including proteases (*2*) and the heme enzyme myeloperoxidase (MPO), which utilizes H_2O_2 and physiological concentrations of Cl^- ions to generate HOCl (*1*). While HOCl and MPO play an important beneficial role in immune defense, they are also strongly implicated in mediating tissue damage that has been observed in a wide range of inflammatory diseases, including atherosclerosis (reviewed in refs *4−6*), cystic fibrosis (*7*, *8*), kidney disease (*9*), and neurodegenerative disorders (*10*).

Over the past few years there has been increasing interest in understanding the reactions of HOCl with biological substrates, primarily as a consequence of the role of HOCl in human diseases. There are now extensive kinetic data for the biological reactions of HOCl (*11−17*; reviewed in refs *18* and *19*), showing that amines and sulfur-containing compounds are major kinetic targets. These functional groups are prevalent in amino acids, peptides, and proteins in the form of Lys, His, Cys, and Met side chains. Proteins and α-amino acids are major constituents of most biological systems, including cells, tissue, and biological fluids, rendering them likely targets for HOCl-mediated damage (*20*).

The consequences of protein damage by HOCl have been studied extensively (*21−28*). Typically, facile oxidation of Met and Cys residues is observed, together with widespread formation of chloramines (RR′N−Cl) at higher HOCl concentrations. Modifications to the aromatic side chains are also observed, particularly oxidation of Trp (indolic) residues and chlorination of Tyr (phenolic) side chains. The accumulated kinetic data for these reactions have previously been incorporated into computational kinetic models in an effort to predict the expected HOCl-mediated modifications of proteins of known amino acid composition (*11*, *12*, *18*, *29*). In cases where these models have been compared to the experimental data, there is gross agreement between the data, but typically the consumption of residues such as Trp and Tyr is underestimated, while that for His and Lys is overestimated (*4*, *11*, *12*, *18*). This is probably due to a combination of two factors: (i) secondary reactions of the

* To whom correspondence should be addressed. Telephone: +61-2-8208-8900. Fax: +61-2-9565-5584. E-mail: pattisond@hri.org.au.

[1] Abbreviations: Apo A-I, apolipoprotein A-I; Apo B-100, apolipoprotein B-100; Cl-Tyr, 3-chlorotyrosine; HOCl, the equilibrium mixture of hypochlorous acid and its anion, OCl^-, at physiological pH 7.4; HPLC, high-performance liquid chromatography; IAACl, the imidazole chloramine of 4-imidazoleacetic acid; LDL, low-density lipoproteins; MetS(O), methionine sulfoxide; MPO, myeloperoxidase; TNB, 5-thio-2-nitrobenzoic acid.

initially formed chloramines and (ii) protein tertiary structure, which may be expected to protect some residues, while favoring damage to other sites.

It is well-established that chloramines are major products of HOCl-mediated protein oxidation, with these known to undergo a range of further reactions (reviewed in refs *18*, *28*, and *30*), including hydrolysis (via imines) to form carbonyls (*23*, *31*), one-electron reduction to form nitrogen-centered radicals (*28*, *32*), and chlorine transfer reactions (*33−38*). Carbonyl and radical formation typically leads to modification of the amine moiety, whereas chlorine transfer reactions regenerate the parent amine and result in transfer of damage to other target molecules. There is considerable kinetic evidence available for chlorine transfer reactions of chloramines (reviewed in ref *18*), with imidazole chloramines particularly reactive (*33*). Chlorine transfer reactions from chloramines are believed to be important in the formation of the marker compound, 3-chloro-Tyr (Cl-Tyr) (*39*). Furthermore, slow equilibration of N−Cl bonds in a mixture of primary amines and chloramines (e.g., between Gly and taurine sites) has been demonstrated (*35*), and all of these species react readily with sulfur-containing residues (*36*).

It has been shown that protein structure can influence the reactions of HOCl with proteins. Oxidation of Apo A-I with either reagent HOCl or a more physiologically relevant MPO/H$_2$O$_2$/Cl$^-$ system results in much greater chlorination of one specific Tyr residue (Tyr-192) than the other six Tyr residues in Apo A-I (*21*, *40*). This has been attributed to a number of factors, including (i) chlorine transfer from chloramines generated on a nearby Lys residue (Lys-195) (*21*), (ii) quenching of HOCl by nearby Met residues in the case of other Tyr residues (*24*), or (iii) localized formation of HOCl due to binding between MPO and Apo A-I (*40*). The latter proposal cannot explain the selectivity observed by reagent HOCl but has similarly been postulated to account for the selective oxidation of the α-amino group in Apo B-100 following oxidation of low-density lipoproteins (LDL) by MPO/H$_2$O$_2$/Cl$^-$ (*41*).

In the current work, the consumption of amino acid side chains by HOCl in two small proteins [insulin (5.7 kDa) and lysozyme (14.4 kDa)] has been investigated. Lysozyme is one of the key enzymes released by activated neutrophils and has been shown to be readily inactivated by HOCl (*22*, *42*). Furthermore, these proteins do not contain any free Cys residues and only low levels of Met and Trp (all of which are major kinetic targets for HOCl); the absence of these residues promotes chloramine formation, thereby allowing the effects of chloramine transfer reactions to be studied more readily. To assess the influence of chloramine transfer reactions and protein structure in determining the pattern of amino acid consumption, the data have been compared to those for identical experiments with *N*-acetyl amino acid mixtures that mimic the protein composition. The results suggest that chloramine transfer reactions are important and, even in relatively small proteins, tertiary structure plays a role in determining the outcome of HOCl-mediated protein oxidation. In the light of these data, second-order rate constants have been determined for chloramine reactions with Trp residues, disulfide bonds, and Met sulfoxide [MetS(O); the primary Met oxidation product] to supplement existing kinetic data (*33*, *35−37*; reviewed in ref *18*). These data have been used to extend previous computational models for HOCl-mediated oxidation of proteins with known amino acid composition (*11*, *12*, *18*, *29*). The experimental amino acid consumption observed for insulin and lysozyme is closely predicted using these revised models.

EXPERIMENTAL PROCEDURES

Materials. All chemicals were obtained from Sigma/Aldrich/Fluka (Castle Hill, NSW, Australia) and used as received, with the exception of sodium hypochlorite (in 0.1 M NaOH, low in bromide; BDH Chemicals, Poole, U.K.) and *N*-acetyl-Met sulfoxide (Bachem, Bubendorf, Switzerland). The HOCl was standardized by measuring the absorbance at 292 nm at pH 12 [ϵ_{292}($^-$OCl) = 350 M^{-1} cm^{-1} (*43*)]. All studies (unless otherwise stated) were performed in 0.1 M phosphate buffer (pH 7.4) which was prepared using Milli Q treated water and treated with Chelex resin (Bio-Rad, Hercules, CA) to remove contaminating metal ions. The pH values of solutions were adjusted, where necessary, to pH 7.4 using 100 mM H$_2$SO$_4$ or 100 mM NaOH.

Kinetic Studies. Kinetic studies were undertaken using a Perkin-Elmer Lambda 40 UV/vis spectrometer interfaced to a PC running WinLab and KinLab software. An SFA-20 stopped-flow accessory (Hitech Scientific, Bradford on Avon, U.K.) was utilized to obtain accurate kinetic data when the reactions were complete within 10 min of mixing. In this case data were acquired sequentially at single wavelengths (from 320 to 230 nm, at 10 nm intervals) and later combined to give time-dependent spectral data (see below for details of analysis). For reactions occurring over longer time scales (>10 min) the spectral region from 320 to 220 nm was scanned (960 nm min^{-1}) at regular intervals (between 1 and 30 min) for the duration of the reaction. The cell holder of the UV/vis spectrometer was held at a constant temperature (22 °C) by a Peltier block, and for stopped-flow experiments the temperature of the solutions was also maintained at 22 °C by circulating water from a thermostated water bath. All measurements were taken relative to a 0.1 M phosphate buffer baseline.

Where possible, HOCl was kept as the limiting reagent with at least a 4-fold excess of substrate. For kinetic studies on the Trp model, the concentration of 3-indolepropionic acid was determined spectrophotometrically using the extinction coefficient for Trp at 280 nm (pH 6.5) of ϵ_{280} = 5690 M^{-1} cm^{-1} (*44*). Data were processed both by single wavelength analysis (Origin 7.0552; OriginLab Corp.) and global analysis methods (Specfit, Version 3.0.36; Spectrum Software Associates; see http://www.bio-logic.fr/rapid-kinetics/specfit.html for further details). All reported rate constants are averages of at least five determinations, with errors specified as 95% confidence limits.

Determination of First-Order Rate Constants for Chloramine Decay. The rates of decay of model Lys and His side chain chloramines, or α-amino chloramines, were determined following mixing of a 10:1 excess of substrate over HOCl for *N*-α-acetyl-Lys, 6-aminocaproic acid, and Gly or a 1.1-fold substrate excess over HOCl for 4-imidazole acetic acid and *N*-α-acetyl-His. Aliquots (20 μL) of the solutions were removed at various intervals over 7 days for the *N*-α-acetyl-Lys, 6-aminocaproic acid, and Gly chloramines and over 6 h for the imidazole chloramines before being assayed for chloramine concentration with 5-thio-2-nitrobenzoic acid

(TNB; 1 mL) (*32, 45*). The first-order rate constants for chloramine decay were determined from linear plots of ln-([chloramine]/M) versus time (s), with the gradients corresponding to $-k$ (s^{-1}) for each chloramine studied.

Preparation of N-Acetyl Amino Acid Mixtures To Mimic Insulin and Lysozyme. The amino acid compositions for insulin and lysozyme were obtained from Swissprot (Primary Accession Numbers P01317 and P00698, respectively). Stock solutions of each individual *N*-acetyl amino acid were prepared such that mixing equal volumes of each stock solution yielded the desired amino acid composition. (*N*-α-Acetyl-Cys)$_2$, *N*-α-acetyl-Trp, and *N*-α-acetyl-Tyr were too insoluble to prepare concentrated stock solutions and were dissolved directly into the final *N*-acetyl amino acid mixture. The concentrations of individual *N*-acetyl amino acids in the resulting mixtures deviated by <3% relative to the parent protein composition, as assessed by weighed mass relative to the amino acid compositions.

Preparation of Samples for Total Amino Acid Analysis by HPLC. Insulin, lysozyme, or the corresponding *N*-acetyl amino acid mixtures were incubated with varying molar excesses of HOCl for 24 h at 22 °C or 3 h at 37 °C. Following incubation the samples were freeze-dried in situ to prevent loss of material and redissolved in 150 μL of preprepared 4 M methanesulfonic acid containing 0.2% w/v tryptamine (from Sigma; packaged under Ar). Use of high-purity methanesulfonic acid minimized the interconversion between Met and MetS(O) observed under hydrolysis conditions (*46*). The samples were then hydrolyzed overnight and prepared for analysis by HPLC as described previously (*22, 46*).

HPLC Instrumentation and Methods. The amino acids were separated by HPLC after precolumn derivatization with *o*-phthaldialdehyde reagent (from Sigma; with 2-mercaptoethanol added) for 1 min before injection onto an Ultrasphere ODS column (4.6 mm × 250 mm, 5 μm particle size) from Beckman-Coulter and separation on a Shimadzu HPLC system at 30 °C, 1 mL min^{-1}, using the following gradient: isocratic 95% solvent A and 5% solvent B for 7 min, then to 25% B over 10 min, 50% B over a further 10 min, with isocratic 50% B for 8 min before increasing to 100% B over 5 min, washing with 100% B for 5 min, and then reequilibration to 95% solvent A and 5% solvent B over 10 min. Solvent A contained 50 mM sodium acetate (pH 5.0), 2.5% (v/v) tetrahydrofuran, and 20% (v/v) methanol, and solvent B contained 50 mM sodium acetate, 2.5% (v/v) tetrahydrofuran, and 80% (v/v) methanol. Amino acid derivatives were detected by their fluorescence (RF10A-XL; Shimadzu, Rydalmere, NSW, Australia) at an excitation wavelength of 340 nm and an emission wavelength of 440 nm and quantified by comparison with amino acid standards [500 μM stock solution from Sigma with MetS(O) added].

Computational Modeling. The computational modeling studies to predict the reactions of HOCl with insulin and lysozyme were undertaken using Specfit software and based on previous computational models (*11*). The amino acid concentrations were taken to model the experimental conditions used, and reactions were simulated both over a 24 h time scale and a time scale that resulted in full chloramine consumption. The models were calculated using 10^3 or 10^4 time points depending on the duration of the simulated reactions, and a log time scale was used to ensure accurate

predictions at both short (HOCl consumption) and long (chloramine reactions) time scales.

Statistical Analysis. All statistical analyses were performed using GraphPad Prism 4 (GraphPad Software, San Diego, CA), with $p < 0.05$ taken as significant. Statistical analyses to compare the effect of HOCl treatment to the untreated controls were carried out using one-way ANOVA with Dunnett's post hoc test. Statistical analyses to compare the extent of amino acid consumption in proteins versus the corresponding *N*-acetyl amino acid mixtures were performed using two-way ANOVA with Bonferroni post hoc testing.

RESULTS

Experimental Analysis of HOCl-Mediated Amino Acid Consumption. The role of protein tertiary structure in determining the pattern of HOCl-mediated protein oxidation has been investigated by examining the extent of amino acid oxidation/modification in insulin and lysozyme and in mixtures of *N*-acetyl amino acids that mimic the protein amino acid composition. *N*-Acetyl-blocked amino acid residues were utilized to prevent reaction of HOCl with the reactive α-amino sites and to provide model peptide bonds as potential targets of HOCl. Free Gly was added to the mixtures at concentrations consistent with those for the N-terminal amine in the protein. It was assumed that any differences observed in the amino acid consumption for proteins versus the protected amino acid solutions on treatment with HOCl could be attributed to protein tertiary structure.

(*i*) *For Insulin and N-Acetyl Amino Acid Mixtures That Mimic Insulin.* The extent of modification of the amino acids (with the exception of cystine) in insulin (0.5 mg mL^{-1}, 34.7 μM) and in corresponding *N*-acetyl amino acid mixtures following exposure (3 h, 37 °C) to increasing molar excesses of HOCl (0−25-fold over protein) is shown in Figure 1.

In the *N*-acetyl amino acid mixtures there was no significant loss of His, Lys, or Arg residues (i.e., those that might be expected to yield chloramines) relative to the controls with no oxidant, although there was a trend toward loss of Lys (Figure 1). For the insulin samples, there was no significant loss of Lys at any molar excesses of oxidant relative to the nonoxidant control. However, significant losses of both His and Arg residues were observed when insulin was treated with a 25-fold molar excess of HOCl but not at lower oxidant concentrations. Direct comparison of the two sets of data by two-way ANOVA (Figure 1) showed significant increases in the consumption of His and Arg residues in insulin compared to the *N*-acetyl amino acid mixture with a 25-fold HOCl excess, but not under other conditions. There were no significant differences in the consumption of Lys residues between insulin and the *N*-acetyl amino acid mixture.

The pattern of Tyr loss (Figure 1) was markedly different between insulin and the corresponding *N*-acetyl amino acid mixture. In both cases significant loss of Tyr was observed with a >10-fold molar excess of HOCl. Interestingly, the loss of Tyr was much greater in the protein samples than in the *N*-acetyl amino acid mixtures, as assessed by two-way ANOVA (Figure 1). There was also a significant difference between the Tyr consumption in insulin and the *N*-acetyl amino acid mixture at an oxidant excess of 5:1 (Figure 1),
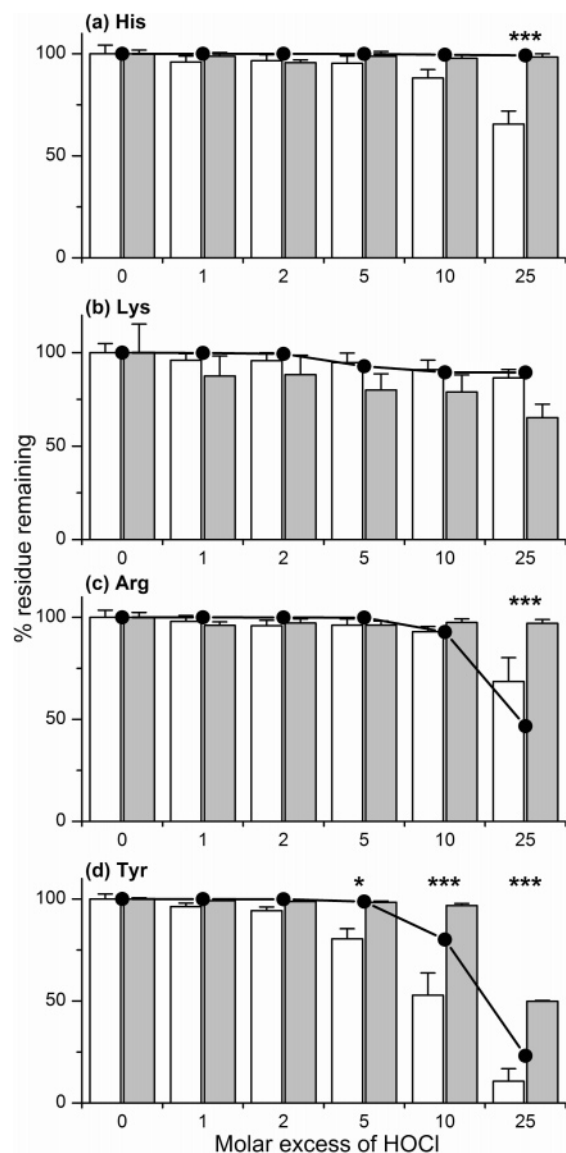
FIGURE 1: Amino acid analysis showing the consumption of (a) His, (b) Lys, (c) Arg, and (d) Tyr following treatment of insulin (0.5 mg mL^{-1}, 87.2 μM; white bars) or corresponding *N*-acetyl amino acid mixtures to mimic insulin composition (gray bars) following incubation with a 0−25-fold molar excess of HOCl for 3 h at 37 °C. The predicted consumption data for each amino acid after 24 h at 22 °C using the computational kinetic model (see Table 4 and Table S1) are also shown (●). Statistically significant differences between the data for insulin and the corresponding *N*-acetyl amino acid mixture with $p < 0.05$ (*), $p < 0.01$ (**), and $p < 0.001$ (***) as assessed by two-way ANOVA are indicated. Data are the mean ± standard error of the mean for four or more experiments.

even though neither of these losses were significant compared to the corresponding nonoxidant controls. It was not possible to assess the oxidation/consumption of cystine residues, although they may be a major target (*18, 28*), as these are destroyed by acid hydrolysis.

(ii) For Lysozyme and N-Acetyl Amino Acid Mixtures That Mimic Lysozyme. The HOCl-induced (0−25-fold molar excess over protein) consumption of amino acid residues in lysozyme (0.5 mg mL^{-1}, 87.2 μM) and the corresponding *N*-acetyl amino acid mixture was investigated over 24 h at 22 °C (Figure 2) and at 37 °C for 3 h; there were no significant differences between the results obtained under these two different incubation conditions.

For the *N*-acetyl amino acid mixture there was no significant loss of His, Lys, or Arg residues relative to control at any excess of oxidant, though there was a trend toward loss of Lys. Similarly, in lysozyme no significant loss of Arg was observed, but significant loss of both His and Lys residues was observed in the protein at higher oxidant excesses (>5-fold for His and at 25-fold for Lys). Comparison of the protein and *N*-acetyl amino acid data by two-way ANOVA showed no significant differences in Arg loss but revealed significantly greater losses of His and Lys in lysozyme than the *N*-acetyl amino acid mixture at high excesses of HOCl (Figure 2).

In both lysozyme and the *N*-acetyl amino acid mixture, significant loss of Trp was observed relative to the controls for all HOCl excesses >5-fold. Trp was almost totally consumed at a 25-fold molar excess of HOCl, and there were no significant differences detected between the lysozyme and *N*-acetyl amino acid mixture (Figure 2). In contrast, while there was no significant loss of Tyr residues observed in the *N*-acetyl amino acid mixture even at the highest excess of HOCl, there was significant loss of Tyr residues in lysozyme at ≥5-fold oxidant excess; at a 25-fold excess only ca. 40% of Tyr residues remained (Figure 2). When the consumption of Tyr in lysozyme versus the *N*-acetyl amino acid mixture was compared by two-way ANOVA, there was significantly more consumption in lysozyme at higher oxidant excesses (Figure 2).

Significant consumption of Met was observed for both lysozyme and the *N*-acetyl amino acid mixture, with only 50% remaining with equimolar HOCl and almost total consumption of Met with a 5-fold molar excess of HOCl. There were no significant differences between the lysozyme and *N*-acetyl amino acid data (Figure 2), except at a 2-fold excess, where there was a greater loss in the amino acid mixture.

It is well-established that oxidation of Met results in sulfoxide formation (*22*); the extent of formation of this species was therefore quantified. In both lysozyme and the *N*-acetyl amino acid mixture there were significant increases, compared to the untreated samples, in MetS(O) levels at all excesses of oxidant, consistent with the rapid consumption of Met. At the higher oxidant excesses (e.g., 25-fold) MetS-(O) was further consumed. In the case of the protein, MetS-(O) levels returned almost to baseline, and there was a significant difference between the MetS(O) levels in lysozyme and the *N*-acetyl amino acid mixture at this excess (Figure 2).

Determination of Chloramine Concentrations in Insulin, Lysozyme, and the Corresponding N-Acetyl Amino Acid Mixtures. In light of the observed changes in His, Lys, and Arg residues and the differences between the protein and *N*-acetyl amino acid mixtures, the concentration of chloramines/amides generated on these residues was assessed, particularly as it has been shown that protein chloramines are typically less stable than those of isolated amino acids (*32*).

For insulin, at all excesses of HOCl investigated, there were significantly greater levels of chloramines/amides present (following incubation for 3 h at 37 °C) in the *N*-acetyl amino acid mixture than in the protein samples (Figure 3a), with the latter being essentially baseline levels (<2% of the added HOCl) at all molar excesses of HOCl. However, for
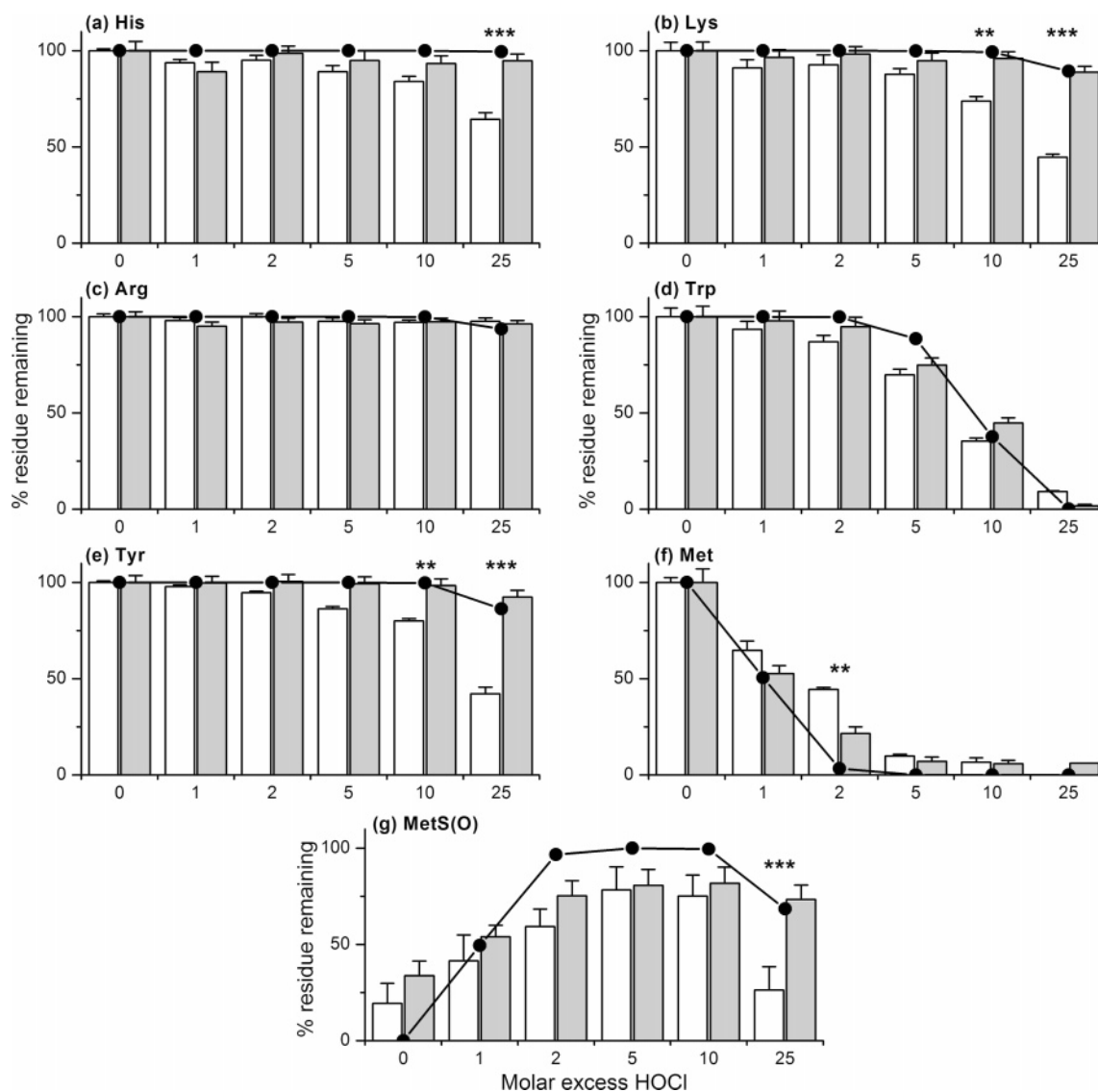
FIGURE 2: Amino acid analysis showing the consumption of (a) His, (b) Lys, (c) Arg, (d) Trp, (e) Tyr, (f) Met, and (g) MetS(O) [shown as the percentage of MetS(O) relative to [Met + MetS(O)] in the control samples] following treatment of lysozyme (0.5 mg mL^{-1}, 34.7 μM; white bars) or corresponding *N*-acetyl amino acid mixtures to mimic lysozyme composition (gray bars) following incubation with a 0−25-fold molar excess of HOCl for 24 h at 22 °C. The predicted consumption data for each amino acid after 24 h at 22 °C using the computational kinetic model (see Table 4 and Table S1) are also shown (●). Statistically significant differences between the data for lysozyme and the corresponding *N*-acetyl amino acid mixture with $p < 0.05$ (*), $p < 0.01$ (**), and $p < 0.001$ (***) as assessed by two-way ANOVA are indicated. Data are the mean ± standard error of the mean for four or more experiments.

the *N*-acetyl amino acid mixtures, 25% of the added HOCl remained as TNB-active material, after 3 h at 37 °C, with equimolar HOCl. While the absolute chloramine/amide concentration increased at higher HOCl excesses (Figure 3a), the proportion of added oxidant remaining as TNB-active material dropped to ca. 3% at a 25-fold HOCl excess.

For lysozyme and the *N*-acetyl amino acid samples with low excesses of HOCl (≤5:1) the absolute levels of chloramines/amides detected after 3 h incubation at 37 °C were close to zero (Figure 3c). At higher oxidant excesses a buildup of chloramines was detected for the *N*-acetyl amino acid mixture but not lysozyme (Figure 3c). This is likely to be due to the reduced stability of protein chloramines (*32*), as seen with insulin, but may also be due to inefficient quantification of lysozyme chloramines/amides due to precipitation of the protein at high excesses of HOCl. Similar trends were observed following a 24 h incubation at 22 °C (Figure 3b), but the absolute levels of chloramine detected in the *N*-acetyl

amino acid mixtures (with HOCl excesses ≥5) were significantly lower than those measured following incubation for 3 h at 37 °C (Figure 3c); this is consistent with the thermal instability of chloramines (*32*).

The differences in chloramine concentrations between the proteins and the *N*-acetyl amino acid mixtures are consistent with the hypothesis that secondary reactions of chloramines play a role in determining the pattern of amino acid consumption in proteins. The reaction kinetics for His side chain chloramines are well-established (*33*), but kinetic studies on the less reactive chloramines of the Lys side chain and the α-amino group of Gly (*18*, *35*, *36*) are incomplete; the studies described below address these omissions.

Kinetics of Tryptophan Side Chain Oxidation by Lys and Gly Chloramines. The reactions of *N*-α-acetyl-Lys and Gly chloramines (25, 50, or 125 μM, to ensure excess substrate) with 3-indolepropionic acid (80−550 μM) were investigated as a model for chloramine-mediated damage to the Trp side
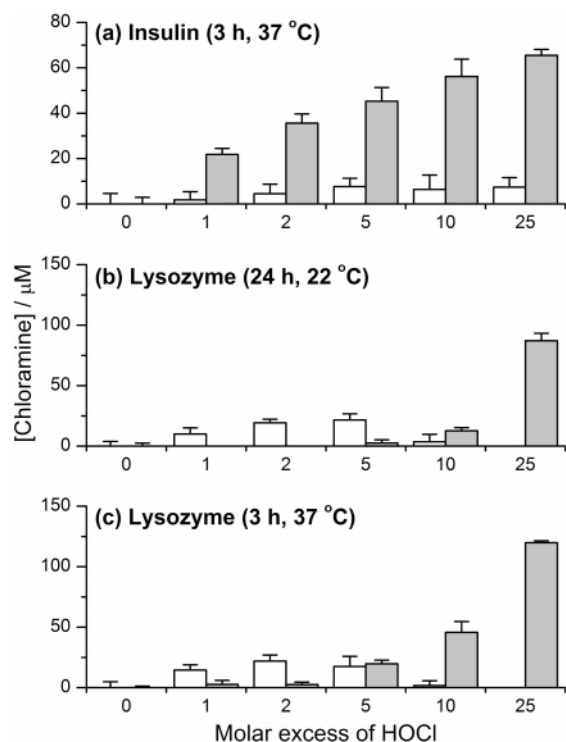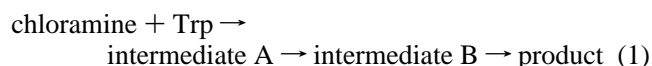
FIGURE 3: Chloramine concentrations measured in protein (white bars) or corresponding *N*-acetyl amino acid mixtures to mimic protein composition (gray bars) following incubation with a 0−25-fold molar excess of HOCl for the prescribed time and temperature: (a) insulin (0.5 mg mL^{-1}, 87.2 μM) after 3 h at 37 °C; (b) lysozyme (0.5 mg mL^{-1}, 34.7 μM) after 24 h at 22 °C; and (c) lysozyme (0.5 mg mL^{-1}, 34.7 μM) after 3 h at 37 °C.
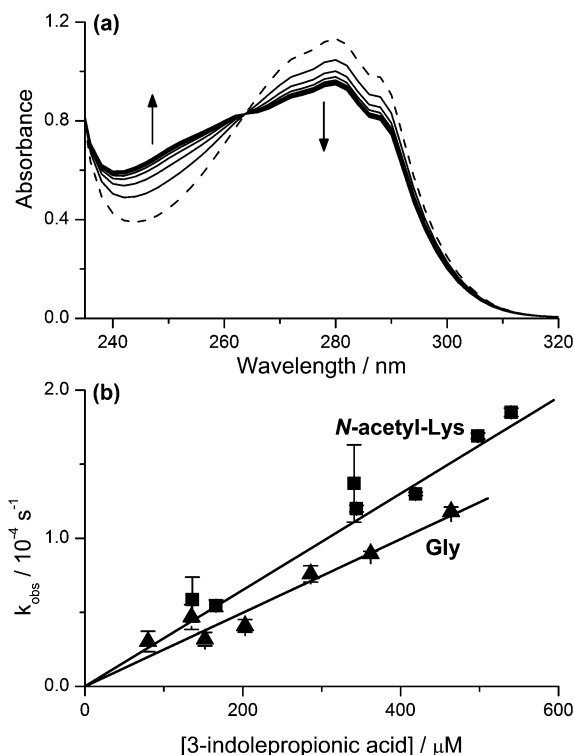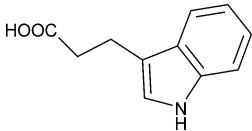

FIGURE 4: Kinetic data for the oxidation of 3-indolepropionic acid (a model of the Trp side chain) with the chloramines of *N*-α-acetyl-Lys and Gly. (a) Absorbance changes observed over 12 h following mixing of 3-indolepropionic acid (500 μM) with *N*-α-acetyl-Lys chloramine (125 μM) at 22 °C and pH 7.4. The spectrum obtained at $t = 0$ h is shown as a dotted line, with subsequent spectra shown at 1 h intervals (the arrows indicate the direction of absorbance change). (b) Linear analysis of the observed pseudo-first-order rate constants against [3-indolepropionic acid] for *N*-α-acetyl-Lys (■) and Gly (▲) chloramines. The gradients of the linear fits correspond to the second-order rate constants given in Table 1. For each data point, error bars represent standard deviations; where these are not visible, the standard deviation is smaller than the symbol size.

chain. The UV/vis absorbance changes (Figure 4a) were monitored over time periods of up to 18 h (65000 s), or until reaction was complete, with a time interval between consecutive spectra of between 1 and 3 min. Complex absorbance changes were observed over time at 280 nm (λ_{max} for the indole absorption) with an initial absorbance decay followed by a growth. Simpler kinetics were observed at shorter wavelengths (240−260 nm) with an increase in absorbance at these wavelengths. These changes are consistent with those observed previously for Trp oxidation by HOCl and His side chain chloramines and were therefore analyzed by global analysis methods using the same mechanism as previously (eq 1) (*11, 33*). As the chlorine transfer

$$\text{chloramine} + \text{Trp} \rightarrow$$
$$\text{intermediate A} \rightarrow \text{intermediate B} \rightarrow \text{product} \quad (1)$$

rates are much slower for these chloramines than HOCl, the steady-state concentration of intermediate A remains low throughout the reaction. Thus, the first-order rate constant for conversion of intermediate A to intermediate B was fixed to that obtained previously (0.1 s^{-1}) (*11*) to reduce the parametrization of the fitting process. This allowed the second-order rate constants for reaction of chloramines with the Trp side chain to be determined accurately, as shown in Table 1.

These rate constants were verified by an alternative analysis, averaging the k_{obs} values obtained by single exponential analysis at individual wavelengths in the range 240−290 nm. Plots of k_{obs} against [3-indolepropionic acid] yielded straight lines, with the gradients equal to the second-

order rate constant for the appearance of the final reaction product. In these experiments, these derived second-order rate constants are equivalent to that for the initial reaction of chloramines with the Trp side chains (Figure 4b, Table 1), as the low reactant concentrations mean that the initial oxidation process is the rate-determining step, consistent with the global analysis fits.

Kinetics of Disulfide Bond Oxidation by Lys and Gly Chloramines. The rates of oxidation of disulfide bonds by *N*-α-acetyl-Lys and Gly chloramines (0.25, 0.5, or 1.0 mM, to ensure excess substrate) were investigated by reaction with 3,3′-dithiodipropionic acid (1.0−4.0 mM). At zero time, a strong absorption band was observed with $\lambda_{max} = 248$ nm, which was attributed to the absorbance of 3,3′-dithiodipropionic acid. Over time (from 0.5 to 2.5 h depending on the substrate concentration) the absorbance maximum shifted to lower wavelength (λ_{max}, 244 nm) with simple exponential kinetics observed either side of the absorbance maxima. Global analysis of these data using a simple mechanism (chloramine + disulfide → product) yielded the second-order rate constants given in Table 1.
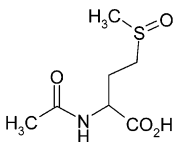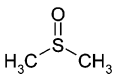
The data were also analyzed by plotting the average k_{obs} values obtained from single wavelength analysis against [3,3′-dithiodipropionic acid]. At lower concentrations of 3,3′-dithiodipropionic acid (1.0−4.0 mM) a linear relationship

Table 1: Second-Order Rate Constants (with 95% Confidence Limits) at 22 °C and pH 7.4 (in 0.1 M Phosphate Buffer) for Reactions of N-α-Acetyl-Lys and Gly Chloramines with Disulfide Bonds and a Trp Side Chain Model

substrate	structure	k_2 (N-α-acetyl-LysCl)/$M^{-1}s^{-1}$	k_2 (GlyCl)/$M^{-1}s^{-1}$
3-indolepropionic acid		0.4 ± 0.1^a 0.33 ± 0.02^b	0.23 ± 0.04^a 0.25 ± 0.01^b
3,3′-dithiodipropionic acid	HOOCCH$_2$CH$_2$S$-$SCH$_2$CH$_2$COOH	0.10 ± 0.02^a 0.14 ± 0.01^b	$0.7 \pm 0. 1^a$ 0.68 ± 0.01^b

^{a} Determined by global analysis. ^{b} Determined by single wavelength analysis.

Table 2: Second-Order Rate Constants (with 95% Confidence Limits) at 22 °C and pH 7.4 (in 0.1 M Phosphate Buffer) for Reactions of HOCl and 4-Imidazoleacetic Acid Chloramine (IAACl; a His Side Chain Model) with Models of Methionine Sulfoxide

substrate	structure	k_2 (HOCl)/ $M^{-1}s^{-1}$	k_2 (IAACl)/ $M^{-1}s^{-1}$
N-acetyl Met sulfoxide		170 ± 10^a 180 ± 10^b	nd
dimethyl sulfoxide		135 ± 5^a 134 ± 4^b	3.6 ± 1.2^a

^{a} Determined by global analysis. ^{b} Determined by single wavelength analysis; nd, not determined.

was obtained, yielding the second-order rate constants shown in Table 1 that are consistent with those obtained by global analysis. However, at high 3,3′-dithiodipropionic acid concentrations (>5 mM) there was a deviation from linearity with an increase in the observed rate constants relative to those expected from the lower concentration data; the cause of this phenomenon remains unclear.

Kinetics of Methionine Sulfoxide Oxidation by HOCl and His Side Chain Chloramines. The amino acid consumption data reported above indicate that Met is readily oxidized to MetS(O), but further oxidation of MetS(O) also occurs at >25-fold molar excesses of HOCl, as has been observed previously (*22*). The second-order rate constant for such secondary oxidation has been measured here due to the potential significance of this reaction, as MetS(O) is readily formed at low excesses of HOCl. The kinetics of oxidation of MetS(O) by HOCl have been investigated using N-acetyl-Met sulfoxide and DMSO. The consumption of HOCl (250 μM) by N-acetyl-Met sulfoxide (0.65−5.8 mM) was monitored from 260 to 320 nm [λ_{max}(HOCl) = 292 nm] and displayed simple exponential kinetics over 30−60 s time scales. The data were analyzed with a simple mechanism [HOCl + MetS(O) → product] by global analysis to yield the second-order rate constant given in Table 2. The data were also analyzed by single wavelength analysis methods, with good agreement between the derived second-order rate constants (Table 2). The reaction of HOCl (250 μM) with DMSO (1.3−10 mM) could be monitored from 220 to 320 nm, as DMSO absorbs only weakly at these wavelengths, unlike the N-acetyl group of N-acetyl-Met sulfoxide. The data were analyzed as described for N-acetyl-Met sulfoxide

with excellent agreement between the single wavelength and global analysis methods (Table 2).

The reactions of the highly reactive His side chain chloramines with MetS(O) models were also investigated. The reaction of 4-imidazoleacetic acid chloramine (IAACl; 250 μM) with DMSO (0.5−25.0 mM) occurred over longer time scales (3−15 min) than those for the HOCl reactions and yielded data that required analysis by a more complex mechanism (IAACl + DMSO → intermediate → dimethylsulfone) than the HOCl data. The second-order rate constant for the initial reaction of the chloramine with DMSO was obtained by global analysis (Table 2). However, as the decays are nonexponential, the second-order rate constant could not be verified by single wavelength analysis. The identity of the intermediate was not investigated further but might be expected to be a chlorinated species such as CH$_3$S(O)(Cl)-CH$_3$. The reactions of IAACl with N-acetyl-Met sulfoxide, and those of N-α-acetyl-His chloramines with N-acetyl-Met sulfoxide and DMSO, could not be accurately assessed as the absorbance of the N-acetyl group obscures the small absorbance changes due to the loss of the imidazole chloramine (230−240 nm).

Determination of Decomposition Rates for Chloramines of Lys and His Side Chains and Gly. The first-order rate constants for chloramine decomposition were assessed by preparing the chloramines (ca. 450 μM) of ϵ-amino-n-caproic acid, N-α-acetyl-Lys (both Lys side chain models), 4-imidazoleacetic acid, N-α-acetyl-His (both His side chain models), and Gly (an α-amino group model). Those for the Lys side chain and α-amino group were prepared with a 10-fold molar excess of amine over HOCl to prevent the formation of dichloramines. As it has been established that His side chain chloramines decompose much more rapidly when there is an excess of substrate (Summers and Hawkins, unpublished results; *47*), His side chain chloramine solutions were prepared with a 1.1-fold molar excess of imidazole over HOCl. The solutions were maintained at 22 °C for 7 days for the Lys and Gly chloramines and for 24 h for the His side chain chloramines. At appropriate time intervals (between 30 min and 24 h depending on the chloramine investigated) the chloramine concentration was determined by removing aliquots of the solutions and assaying with TNB. The data were plotted as ln[chloramine] against time, yielding linear plots with gradients corresponding to $-k$, where k is the first-order rate constant for decomposition under these conditions (see Figure 5 and Table 3).

Computational Modeling Predictions for the Reactions of HOCl with Insulin and Lysozyme. The kinetic data accrued previously (*11*, *18*, *33*, *35*, *36*), together with the rate
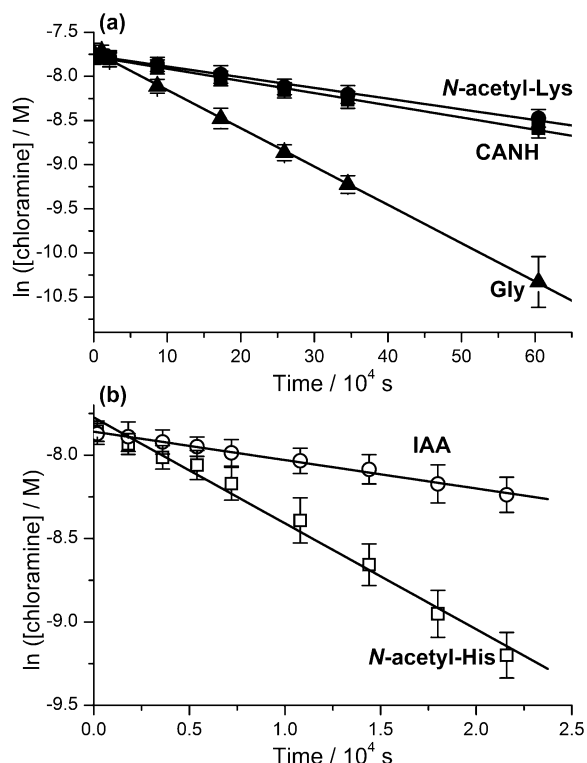
FIGURE 5: Analysis of chloramine stability at pH 7.4 and 22 °C showing linear plots of ln([chloramine]) vs time with the resulting gradients equivalent to $-k$ (as given in Table 3). (a) Models of Lys side chain chloramines [ϵ-amino-n-caproic acid (CANH; ●), N-α-acetyl-Lys (■)] and α-amino groups [Gly (▲)] were prepared with a 10-fold molar excess of HOCl over amine and were assayed over 7 days. (b) Models of His side chain chloramines [4-imidazoleacetic acid (IAA, ○), N-α-acetyl-His (□)] were prepared with a 1.1-fold molar excess of HOCl over imidazole and monitored for 23 h. For each data point, error bars represent standard deviations; where these are not visible, the standard deviation is smaller than the symbol size.

Table 3: First-Order Rate Constants (with 95% Confidence Limits) at 22 °C and pH 7.4 (in 0.1 M Phosphate Buffer) for Decomposition of Model Chloramines of Lys (ϵ-Amino-n-caproic Acid, N-α-Acetyl-Lys) and His (4-Imidazoleacetic Acid, N-α-Acetyl-His) Side Chains and α-Amino Groups (Gly)

chloramine	k/s^{-1}
ϵ-amino-n-caproic acid	$(1.4 \pm 0.1) \times 10^{-6}$
N-α-acetyl-Lys	$(1.2 \pm 0.1) \times 10^{-6}$
4-imidazoleacetic acid	$(1.7 \pm 0.1) \times 10^{-5}$
N-α-acetyl-His	$(6.4 \pm 0.6) \times 10^{-5}$
Gly	$(4.3 \pm 0.1) \times 10^{-6}$

constants determined here, allow the development of a simple computational model to predict the expected fate of HOCl on reaction with proteins. A previous model utilized the rate constants for reactions of HOCl with protein components to predict the initial sites of HOCl damage on proteins (*11*) but did not consider the secondary reactions of chloramines (reviewed in refs *18* and *28*). The reactions and the kinetic parameters incorporated into the latest model are given in the Supporting Information (Table S1). The kinetic parameters for the initial HOCl reactions are identical to those used for the original computational model (*11*). The second-order rate constants used for the secondary reactions of His (imidazole) chloramines are taken from a previous study (*33*). The rate constants for the chlorination of the Tyr side chain by Lys and α-amino chloramines are very slow and have

Table 4: Protein Composition Data Used for Computational Kinetic Model for Reaction of Insulin (0.5 mg mL^{-1}, 87.2 μM) and Lysozyme (0.5 mg mL^{-1}, 34.7 μM) with HOCl (0–25 Molar Excess over Protein)[a]

amino acid	insulin[b]		lysozyme	
	no. per molecule	[residue]/ μM	no. per molecule	[residue]/ μM
His	2	174.4	1	34.7
Lys	1	87.2	6	208.2
Arg	1	87.2	11	381.7
Asn	3	261.6	14	485.8
Gln	3	261.6	3	104.1
Cys	0	0	0	0
Met	0	0	2	69.4
cystine	3	261.6	4	138.8
Tyr	4	348.8	3	104.1
Trp	0	0	6	208.2
terminal amine	2	174.4	1	34.7
backbone amide	51	4447.2	129	4476.3

[a] See Supporting Information for reactions and kinetic parameters incorporated into the model (Table S1). [b] Insulin exists as a disulfide-linked dimer of the A and B chains.

been estimated using the yields of chlorinated N-acetyl-Tyr following full decomposition of the chloramines (*33*) and comparing this to the decomposition rates determined here. Other rate constants for chloramine transfer reactions have been taken from the studies of Peskin et al. (*35, 36*), with the rate constants for chlorine transfer between Lys side chain and α-amino sites estimated from data for interconversion of Tau, histamine, and Gly chloramines (*35*).

The computational models were completed by combining the kinetic data with the amino acid composition data (Table 4) for insulin (Swissprot Primary Accession Number P01317) and lysozyme (Swissprot Primary Accession Number P00698) to investigate how protein composition affects the pattern of HOCl-mediated damage to proteins.

The model predictions for amino acid consumption in insulin and lysozyme with increasing molar excesses (0–25-fold molar excess over protein) of HOCl are shown overlaid as solid black lines on the experimental consumption data (Figures 1 and 2) for the proteins and corresponding N-acetyl amino acid mixtures. For each amino acid residue the proportion of parent residue predicted to remain after 24 h at 22 °C is shown.

The extent of oxidation of sulfur-containing residues, namely, Met and disulfide bonds, has been predicted in both proteins. Insulin does not contain any Met residues, but the two Met residues in lysozyme are predicted to be almost totally converted (3% remaining) to MetS(O) with only a 2-fold molar excess of HOCl over lysozyme (Figure 2). However, the kinetic studies indicate that MetS(O) can be oxidized further by HOCl to Met sulfone. The modeling data predict that appreciable Met sulfone formation only occurs with a 25-fold molar excess of oxidant over lysozyme (Figure 2), with ca. 30% of Met converted to Met sulfone and the remainder present as MetS(O). The predicted behavior for the oxidation of disulfide bonds in the two proteins is quite different (data not shown). In insulin, it is predicted that only 67% of disulfides remain with equimolar HOCl and insulin, dropping to 35% at a 2-fold excess of HOCl, and are totally consumed by a 5-fold oxidant excess. In contrast, for lysozyme, only minimal disulfide oxidation is predicted at a 2:1 ratio, dropping to only ca. 40% of disulfides remaining

at 5:1 and totally consumed by 10:1. This difference in predicted reactivity is consistent with rapid consumption of HOCl by Met, thereby "protecting" other residues from oxidation until the Met residues are fully consumed.

The side chains of His, Lys, and Arg, the N-terminal amines and peptide bonds, are predicted to be targeted to varying degrees in the two proteins, with these reactions resulting in chloramine formation. In both insulin and lysozyme, no consumption of His residues is predicted after 24 h (Figures 1 and 2), consistent with the rapid chlorine transfer reactions that occur with His chloramines (*33*) and with previous experimental observations (*22*). In both proteins minimal irreversible loss (<10%) of Lys residues (to form carbonyls) is predicted after 24 h with a 25-fold oxidant excess (Figures 1 and 2). However, after 24 h reasonable levels of Lys chloramines are predicted to remain, consistent with the experimental data for the *N*-acetyl amino acid mixtures. When the computational modeling was repeated over longer time scales that allowed complete chloramine decomposition, only ca. 5% of unmodifed Lys residues were predicted to remain in both proteins. Similar patterns of irreversible consumption are predicted for the N-terminal amines (data not shown), with ca. 70% of α-amino groups (or the corresponding chloramine) remaining after 24 h and almost total consumption (presumably to form carbonyl species) once all chloramines have decayed. Low levels of Arg consumption are predicted for lysozyme (Figure 2) and insulin at low molar excesses of HOCl, but substantial Arg loss (ca. 50%) is predicted in insulin with a 25-fold excess of HOCl (Figure 1). These predictions are not altered over longer time scales as transfer reactions to Arg from Lys and α-amino chloramines were not included in the model as they are likely to be slow. Appreciable chlorination of the protein backbone (up to 30% at a 25-fold excess of HOCl) is predicted for insulin, but for lysozyme only low levels (<5%) of backbone chlorination are predicted (data not shown).

The modeling data for the aromatic Tyr and Trp residues in the two proteins show slightly different behavior. For Tyr side chains, it is predicted that, in insulin, only low levels of Tyr chlorination occur up to a 5-fold excess of HOCl, but with a 25-fold oxidant excess ca. 75% of Tyr residues are chlorinated after 24 h (Figure 1); this increases slightly after full decomposition of the chloramines (data not shown). In lysozyme, the predicted extent of Tyr chlorination is much lower (Figure 2), with minimal Cl-Tyr formation predicted with <10-fold HOCl excesses and ca. 15% at a 25-fold excess of HOCl after 24 h. Increasing consumption of Trp in lysozyme is predicted to occur once the oxidant exceeds a 2-fold excess over lysozyme, with almost total consumption predicted at a 25-fold excess (Figure 2).

DISCUSSION

Insulin (51 residues, 5.7 kDa) and lysozyme (129 residues, 14.4 kDa) were chosen as model proteins for these studies, primarily because neither protein contains free thiols (which are major kinetic targets for HOCl) while, in addition, insulin does not contain highly reactive Met or Trp residues. The low content of free Cys, Met, and Trp residues in these proteins enhanced the generation of chloramines, thereby allowing the effects of their subsequent transfer reactions,

for example, to form chlorinated Tyr residues, to be studied more readily.

The extents of amino acid consumption predicted by the computational kinetic models for insulin and lysozyme are in excellent agreement with the experimental data, both for the proteins and for the free *N*-acetyl amino acid mixtures. In some cases deviations from the models are observed, but these can be explained in terms of differing accessibility of residues in proteins and/or chlorine transfer processes following formation of protein-bound Lys and His chloramines. While it is possible that this agreement between experimental and predicted data is a fortuitous coincidence, with the decrease in accessibility of some residues (such as Met and Trp) compensated for by increased rate constants once the residues are incorporated into a protein backbone, it is felt that this scenario is unlikely. Any such increase in rate constants would be expected to occur for all amino acid side chains and would therefore result in greater discrepancies between the model and experimental data than is observed.

It should also be noted that many of the reactions of HOCl are pH dependent, particularly around physiological pH as HOCl has a pK_a of 7.6 (*43*). Thus, factors such as the effective pH in a protein differing to the bulk solution, or the pK_a values for sensitive residues such as Cys and His depending on the local protein environment, may affect their reactivity compared to free amino acids. These factors cannot be readily incorporated into the computational models, but nevertheless there is close agreement between the computational predictions and experimentally observed consumption of the various amino acids.

The enhanced loss of Tyr residues in the proteins versus the *N*-acetyl amino acid mixtures is consistent with previous reports (*21*, *39*) showing that chloramine formation, and subsequent intramolecular chlorine transfer, is a major mechanism of Tyr chlorination in proteins; this confirms previous data for free Tyr (*39*), small peptides, and proteins (*21*). Chlorination of the ring of *N*-α-acetyl-Tyr by isolated chloramines only occurs to a significant extent over a period of several days (*21*, *33*). In contrast, when chloramines were generated on small *N*-acetyl-blocked peptides containing Lys and Tyr residues separated by between 0 and 4 amino acid residues, up to 20% incorporation of chlorine from HOCl into Cl-Tyr occurred within 30 min incubation at 37 °C (*21*). The yield was maximal when the Lys and Tyr residues were separated by two amino acids; this has been attributed to the α-helical structure of the peptides placing the donor and acceptor amino acids in close proximity, thereby facilitating chlorine transfer (*21*). Similar effects would be expected in helices within proteins and also between Lys and Tyr residues that are held in a favorable spatial conformation through tertiary structure.

While Tyr consumption was enhanced in both insulin and lysozyme when compared to the corresponding *N*-acetyl amino acid mixtures, there were no major differences in Trp or Met consumption between lysozyme and the corresponding *N*-acetyl amino acid mixture. Likewise, there was little effect on the extent of MetS(O) formation between the two sets of samples, although there was enhanced consumption of MetS(O) in the protein compared to the free amino acid mixture at high oxidant concentrations.

These observations are somewhat surprising as inspection of the crystal structure of lysozyme shows that the Met

residues are buried within the protein core, where it might be expected that they would be protected, at least to some degree, from oxidation by the water-soluble HOCl. It is possible that protein unfolding occurs following addition of HOCl, thereby exposing Met residues to the solvent, but previous studies have shown that Met oxidation precedes significant protein unfolding (22, 48). The computational models predict that the Met residues are consumed by direct HOCl-mediated oxidation, consistent with the hypothesis that HOCl can readily penetrate into hydrophobic regions of proteins. This has also been confirmed experimentally (22), as there was no time-dependent loss of Met in lysozyme consistent with chloramine transfer reactions. In contrast, overoxidation of Met to Met sulfone is seen more extensively in lysozyme than the corresponding amino acid mixtures, suggesting that chloramine transfer reactions play a role in the oxidation of MetS(O). The computational modeling results support the hypothesis that further oxidation of MetS-(O) is primarily mediated by chloramine reactions.

In contrast to the situation of Met, the crystal structure of lysozyme shows that half of the Trp residues are buried in the hydrophobic core, while the other three residues are relatively solvent-accessible in the active site of the enzyme. It might be expected that these solvent-accessible Trp residues are more readily oxidized than those in the hydrophobic core, but there is no evidence for any biphasic Trp consumption or for any differences between the lysozyme and free N-acetyl amino acid samples. Previous studies have shown that treatment of lysozyme with a 5-fold excess of HOCl causes significant protein unfolding (22), and this may account for the lack of protection of the protein Trp residues relative to the freely diffusing N-acetyl amino acids mixtures. The kinetic modeling calculations predict that chloramine transfer reactions are important in mediating Trp oxidation in lysozyme, and correlations between chloramine decay and Trp loss have been observed (22). However, the lack of enhanced Trp oxidation in the protein samples relative to the free amino acid samples suggests that, while chlorine transfer reactions from His or Lys chloramines are occurring, there are no favorable interactions that promote these transfer processes as seen with Tyr. This is probably due to the increased reactivity of Trp side chains when compared to Tyr side chains.

The levels of His consumption observed in insulin and lysozyme are greater than those observed in their corresponding amino acid mixtures or predicted by the computational models, indicating that there are further His chloramine decomposition pathways that are favored in proteins. These may include the formation of protein cross-links via His residues; this possibility is currently under investigation. Alternatively, the increased His loss in proteins may be due to the formation of chloramines at sites where chlorine transfer cannot occur rapidly, and hence the His chloramines decompose by other pathways, possibly to yield aldehydic products. Similar reactions may account for the increased Lys and Arg consumption observed in the proteins versus the amino acid mixtures or predicted by the computational model. However, reversion of chloramines to the parent amino acids during the hydrolysis procedure cannot be discounted, particularly in the N-acetyl amino acid mixtures where significant chloramine concentrations remain after the incubation period. This is more likely to apply to the stable

Lys and Arg chloramines but is unlikely for His chloramines as they are relatively short-lived (33) and would not be expected to be present after the incubation times used. In the protein samples only low levels of chloramines remain, and therefore reversion to the parent amino acid during hydrolysis must be negligible. Although acid hydrolysis has previously been shown to cause artifactual chlorination of Tyr and Phe residues when chloramines are present [due to Cl_2 formation in the presence of HCl (30, 49)], this does not occur with methanesulfonic acid hydrolysis (30) and is unlikely to be a factor here.

The stability of chloramines is known to be structure dependent (31, 50). The first-order decomposition rate constants determined here are consistent with previous data showing that Lys side chain chloramines have a longer half-life than α-amino chloramines (31). The latter decompose via decarboxylation to an imine intermediate that subsequently hydrolyzes to aldehydes; such reactions are less favored with Lys side chain chloramines due to the absence of the neighboring carboxyl group (23, 31). Chloramine decomposition has been shown to follow first-order kinetics (51, 52), but most data have been obtained at basic pH. The first-order rate constants for decomposition of Leu and 2-aminobutan-1-ol chloramines have been determined at neutral pH and 25 °C as ca. 3×10^{-4} s^{-1} and 1×10^{-6} s^{-1}, respectively (51, 52). The rate constant for 2-aminobutan-1-ol is consistent with that determined here for the Lys side chain, but that for Leu is faster than that determined here for Gly; this may be due to destabilization of the chloramine by the large aliphatic side chain in Leu. The corresponding decomposition reactions of His (imidazole) chloramines have not been identified, although 2-oxo-His is a likely product (reviewed in refs 18 and 28). The reasons for the enhanced rate of decomposition of imidazole chloramines in the presence of excess imidazole are unclear, but are currently under further investigation.

While first-order rate constants for chloramine decomposition have been assessed for isolated species such as N-α-acetyl-Lys, it is known that the lifetimes of protein chloramines are greatly diminished relative to those for free amino acids (32, 50); the data presented here clearly illustrate this effect. This may reflect the presence of other protein targets which are constrained by the three-dimensional structure in close proximity to the chloramine, thereby promoting chlorine transfer reactions; this is consistent with the low protein carbonyl yields detected on HOCl-modified proteins (22, 32, 53). These data suggest that tertiary protein structures promote *intra*molecular reactions of chloramines, when compared to the *inter*molecular transfer reactions of isolated substrates.

Previous kinetic studies of aliphatic chloramines with thiols and Met have yielded rate constants that are typically ca. 5 orders of magnitude slower than those for the corresponding reactions of HOCl (reviewed in ref 18). The second-order rate constants determined in these studies for the reactions of Lys side chain and α-amino chloramines with Trp side chains and disulfide bonds are consistent with this decrease in reactivity, and also with studies (54, 55) that show the formation of moderately stable chloramines on cystine and GSSG, despite the presence of disulfide bonds. It is interesting to note, however, that N-α-acetyl-Lys chloramines oxidize 3-indolepropionic acid more rapidly than Gly

chloramines (Table 1). Gly chloramines are ca. four times more reactive with Met than Lys side chain chloramines (*18*, *36*), whereas for Cys and GSH the two chloramines have similar second-order rate constants. In contrast, the reaction of *N*-α-acetyl-Lys chloramine with ascorbate is approximately twice that of Gly chloramines (*18*, *36*). These changes in the relative reactivities of these two chloramines may be due to the delocalized nature of the electron density on ascorbate and the Trp side chain compared with the nucleophilic side chains of the sulfur-containing substrates.

Interestingly, the plots of k_{obs} against substrate concentration obtained for the reactions of chloramines with the disulfide bonds of 3,3′-dithiodipropionic acid show deviations from linearity at high concentrations of substrate, with k_{obs} becoming larger. This kinetic behavior could not be fitted by exponential or quadratic fits but suggests that, following initial reaction of chloramines with the disulfide bond, there are secondary reactions of the intermediate with further disulfide bonds, which are favored at high disulfide concentrations. This deviation from linearity was only observed with disulfide concentrations much higher than are typically encountered in proteins. Thus only data falling in the linear range (<4.0 mM) have been used to calculate the second-order rate constants listed in Table 1. It is unlikely that the concentrations of disulfide bonds required to observe these nonlinear effects would be achieved in biological fluids or even in localized domains within proteins; thus the mechanism behind this phenomenon has not been investigated further.

The amino acid analysis data show that appreciable concentrations of MetS(O) are generated at low molar excesses of HOCl. The kinetic studies show that further oxidation of this compound by HOCl and imidazole chloramines is slow compared with parent Met. Importantly, however, they are still sufficiently reactive to provide an alternative substrate, for example, to Tyr side chains [k_2(HOCl) = 44 M^{-1} s^{-1} (*11*)]. Previous competitive kinetic studies indicated that the concentration of DMSO must be 2 × 10^5 times higher than that required for Cys to cause identical inhibition of monochlorodimedon chlorination (*14*). This yields k_2(HOCl + DMSO) ∼ 160 M^{-1} s^{-1} when comparing to the second-order rate constant estimated for Cys (*11*), which is in excellent agreement with the absolute rate constant determined here.

In summary, these studies show that chlorine transfer reactions of chloramines are important in HOCl-mediated protein oxidation and that protein tertiary structure plays a role in determining the pattern of oxidative damage to the protein, even in small proteins such as insulin and lysozyme. The experimental amino acid consumption can be accurately modeled in isolated proteins (providing their composition is known) using kinetic parameters for direct HOCl reactions and secondary reactions mediated by chloramines. These studies pertain to relatively low molecular mass species in dilute solutions (0.5 mg mL^{-1}). The protein concentration in biological fluids such as plasma is considerably higher [ca. 70 mg mL^{-1} (*56*)]; this would be expected to favor chloramine transfer reactions between proteins, thereby reducing the formation of chloramine decomposition products such as 2-oxo-His and other carbonyls.

SUPPORTING INFORMATION AVAILABLE

The reactions and corresponding rate constants used to define the computational models for the reactions of HOCl with insulin and lysozyme (Table S1). This material is available free of charge via the Internet at http://pubs.acs.org.

REFERENCES

1. Klebanoff, S. J. (1999) Myeloperoxidase, *Proc. Assoc. Am. Phys. 111*, 383−389.
2. Klebanoff, S. J. (2005) Myeloperoxidase: Friend and foe, *J. Leukocyte Biol. 77*, 598−625.
3. Babior, B. M. (1987) The respiratory burst oxidase, *Trends Biochem. Sci. 12*, 241−243.
4. Malle, E., Marsche, G., Arnhold, J., and Davies, M. J. (2006) Modification of low-density lipoprotein by myeloperoxidase-derived oxidants and reagent hypochlorous acid, *Biochim. Biophys. Acta 1761*, 392−415.
5. Podrez, E. A., Abu-Soud, H. M., and Hazen, S. L. (2000) Myeloperoxidase-generated oxidants and atherosclerosis, *Free Radical Biol. Med. 28*, 1717−1725.
6. Stocker, R., and Keaney, J. F., Jr. (2004) Role of oxidative modifications in atherosclerosis, *Physiol. Rev. 84*, 1381−1478.
7. Kettle, A. J., Chan, T., Osberg, I., Senthilmohan, R., Chapman, A. L., Mocatta, T. J., and Wagener, J. S. (2004) Myeloperoxidase and protein oxidation in the airways of young children with cystic fibrosis, *Am. J. Respir. Crit. Care Med. 170*, 1317−1323.
8. van der Vliet, A., Nguyen, M. N., Shigenaga, M. K., Eiserich, J. P., Marelich, G. P., and Cross, C. E. (2000) Myeloperoxidase and protein oxidation in cystic fibrosis, *Am. J. Physiol. Lung Cell. Mol. Physiol. 279*, L537−L546.
9. Malle, E., Buch, T., and Grone, H.-J. (2003) Myeloperoxidase in kidney disease, *Kidney Int. 64*, 1956−1967.
10. Yap, Y. W., Whiteman, M., and Cheung, N. S. (2007) Chlorinative stress: An under appreciated mediator of neurodegeneration?, *Cell. Signalling 19*, 219−228.
11. Pattison, D. I., and Davies, M. J. (2001) Absolute rate constants for the reaction of hypochlorous acid with protein side-chains and peptide bonds, *Chem. Res. Toxicol. 14*, 1453−1464.
12. Pattison, D. I., Hawkins, C. L., and Davies, M. J. (2003) Hypochlorous acid mediated oxidation of lipid components and antioxidants present in low density lipoproteins: Absolute rate constants, product analysis and computational modeling, *Chem. Res. Toxicol. 16*, 439−449.
13. Folkes, L. K., Candeias, L. P., and Wardman, P. (1995) Kinetics and mechanisms of hypochlorous acid reactions, *Arch. Biochem. Biophys. 323*, 120−126.
14. Winterbourn, C. C. (1985) Comparative reactivities of various biological compounds with myeloperoxidase-hydrogen peroxide-chloride, and similarity of the oxidant to hypochlorite, *Biochim. Biophys. Acta 840*, 204−210.
15. Armesto, X. L., Canle, M., Fernandez, M. I., Garcia, M. V., and Santaballa, J. A. (2000) First steps in the oxidation of sulfur-containing amino acids by hypohalogenation: Very fast generation of intermediate sulfenyl halides and halosulfonium cations, *Tetrahedron 56*, 1103−1109.
16. Armesto, X. L., Canle, L., and Santaballa, J. A. (1993) α-Amino acids chlorination in aqueous media, *Tetrahedron 49*, 275−284.
17. Prutz, W. A. (1996) Hypochlorous acid interactions with thiols, nucleotides, DNA, and other biological substrates, *Arch. Biochem. Biophys. 332*, 110−120.
18. Pattison, D. I., and Davies, M. J. (2006) Reactions of myeloperoxidase-derived oxidants with biological substrates: Gaining chemical insight into human inflammatory diseases, *Curr. Med. Chem. 13*, 3271−3290.
19. Armesto, X. L., Canle, M., Garcia, M. V., and Santaballa, J. A. (1998) Aqueous chemistry of *N*-halo-compounds, *Chem. Soc. Rev. 27*, 453−460.
20. Davies, M. J. (2005) The oxidative environment and protein damage, *Biochim. Biophys. Acta 1703*, 93−109.

21. Bergt, C., Fu, X., Huq, N. P., Kao, J., and Heinecke, J. W. (2004) Lysine residues direct the chlorination of tyrosines in YXXK motifs of apolipoprotein A-I when hypochlorous acid oxidizes HDL, *J. Biol. Chem. 279*, 7856−7866.

22. Hawkins, C. L., and Davies, M. J. (2005) Inactivation of protease inhibitors and lysozyme by hypochlorous acid: Role of side-chain oxidation and protein unfolding in loss of biological function, *Chem. Res. Toxicol. 18*, 1600−1610.

23. Peng, D. Q., Wu, Z. P., Brubaker, G., Zheng, L. M., Settle, M., Gross, E., Kinter, M., Hazen, S. L., and Smith, J. D. (2005) Tyrosine modification is not required for myeloperoxidase-induced loss of apolipoprotein A-I functional activities, *J. Biol. Chem. 280*, 22775−22784.

24. Shao, B., Oda, M. N., Bergt, C., Fu, X., Green, P. S., Brot, N., Oram, J. F., and Heinecke, J. W. (2006) Myeloperoxidase impairs ABCA1-dependent cholesterol efflux through methionine oxidation and site-specific tyrosine chlorination of apolipoprotein A-I, *J. Biol. Chem. 281*, 9001−9005.

25. Zheng, L., Nukuna, B., Brennan, M. L., Sun, M., Goormastic, M., Settle, M., Schmitt, D., Fu, X., Thomson, L., Fox, P. L., Ischiropoulos, H., Smith, J. D., Kinter, M., and Hazen, S. L. (2004) Apolipoprotein A-I is a selective target for myeloperoxidase-catalyzed oxidation and functional impairment in subjects with cardiovascular disease, *J. Clin. Invest. 114*, 529−541.

26. Peskin, A. V., and Winterbourn, C. C. (2006) Taurine chloramine is more selective than hypochlorous acid at targeting critical cysteines and inactivating creatine kinase and glyceraldehyde-3-phosphate dehydrogenase, *Free Radical Biol. Med. 40*, 45−53.

27. Fu, X., Kao, J. L. F., Bergt, C., Kassim, S. Y., Huq, N. P., d'Avignon, A., Parks, W. C., Mecham, R. P., and Heinecke, J. W. (2004) Oxidative cross-linking of tryptophan to glycine restrains matrix metalloproteinase activity: Specific structural motifs control protein oxidation, *J. Biol. Chem. 279*, 6209−6212.

28. Hawkins, C. L., Pattison, D. I., and Davies, M. J. (2003) Hypochlorite-induced oxidation of amino acids, peptides and proteins, *Amino Acids 25*, 259−274.

29. Rees, M. D., Pattison, D. I., and Davies, M. J. (2005) Oxidation of heparan sulphate by hypochlorite: Role of *N*-chloro derivatives and dichloramine-dependent fragmentation, *Biochem. J. 391*, 125−134.

30. Winterbourn, C. C., and Kettle, A. J. (2000) Biomarkers of myeloperoxidase-derived hypochlorous acid, *Free Radical Biol. Med. 29*, 403−409.

31. Hazen, S. L., d'Avignon, A., Anderson, M. A., Hsu, F. F., and Heinecke, J. W. (1998) Human neutrophils employ the myeloperoxidase-hydrogen peroxide-chloride system to oxidize α-amino-acids to a family of reactive aldehydes, *J. Biol. Chem. 273*, 4997−5005.

32. Hawkins, C. L., and Davies, M. J. (1998) Hypochlorite-induced damage to proteins: Formation of nitrogen-centred radicals from lysine residues and their role in protein fragmentation, *Biochem. J. 332*, 617−625.

33. Pattison, D. I., and Davies, M. J. (2005) Kinetic analysis of the role of histidine chloramines in hypochlorous acid mediated protein oxidation, *Biochemistry 44*, 7378−7387.

34. Pattison, D. I., and Davies, M. J. (2006) Evidence for rapid inter- and intra-molecular chlorine transfer reactions of histamine and carnosine chloramines: Implications for the prevention of hypochlorous acid mediated damage, *Biochemistry 45*, 8152−8162.

35. Peskin, A. V., Midwinter, R. G., Harwood, D. T., and Winterbourn, C. C. (2004) Chlorine transfer between glycine, taurine and histamine: Reaction rates and impact on cellular reactivity, *Free Radical Biol. Med. 37*, 1622−1630.

36. Peskin, A. V., and Winterbourn, C. C. (2001) Kinetics of the reactions of hypochlorous acid and amino acid chloramines with thiols, methionine, and ascorbate, *Free Radical Biol. Med. 30*, 572−579.

37. Prutz, W. A. (1999) Consecutive halogen transfer between various functional groups induced by reaction of hypohalous acids: NADH oxidation by halogenated amide groups, *Arch. Biochem. Biophys. 371*, 107−114.

38. Prutz, W. A. (1998) Interactions of hypochlorous acid with pyrimidine nucleotides, and secondary reactions of chlorinated pyrimidines with GSH, NADH, and other substrates, *Arch. Biochem. Biophys. 349*, 183−191.

39. Domigan, N. M., Charlton, T. S., Duncan, M. W., Winterbourn, C. C., and Kettle, A. J. (1995) Chlorination of tyrosyl residues in peptides by myeloperoxidase and human neutrophils, *J. Biol. Chem. 270*, 16542−16548.

40. Zheng, L., Settle, M., Brubaker, G., Schmitt, D., Hazen, S. L., Smith, J. D., and Kinter, M. (2005) Localization of nitration and chlorination sites on apolipoprotein A-I catalyzed by myeloperoxidase in human atheroma and associated oxidative impairment in ABCA1-dependent cholesterol efflux from macrophages, *J. Biol. Chem. 280*, 38−47.

41. Yang, C. Y., Wang, J., Krutchinsky, A. N., Chait, B. T., Morrisett, J. D., and Smith, C. V. (2001) Selective oxidation in vitro by myeloperoxidase of the *N*-terminal amine in apolipoprotein B-100, *J. Lipid Res. 42*, 1891−1896.

42. Vissers, M. C., and Winterbourn, C. C. (1987) Myeloperoxidase-dependent oxidative inactivation of neutrophil neutral proteinases and microbicidal enzymes, *Biochem. J. 245*, 277−280.

43. Morris, J. C. (1966) The acid ionization constant of HOCl from 5 °C to 35 °C, *J. Phys. Chem. 70*, 3798−3805.

44. Gill, S. C., and von Hippel, P. H. (1989) Calculation of protein extinction coefficients from amino acid sequence data, *Anal. Biochem. 182*, 319−326.

45. Thomas, E. L., Grisham, M. B., and Jefferson, M. M. (1986) Preparation and characterization of chloramines, *Methods Enzymol. 132*, 569−585.

46. Morgan, P. E., Sturgess, A. D., and Davies, M. J. (2005) Increased levels of serum protein oxidation and correlation with disease activity in systemic lupus erythematosus, *Arthritis Rheum. 52*, 2069−2079.

47. Peskin, A. V., and Winterbourn, C. C. (2003) Histamine chloramine reactivity with thiol compounds, ascorbate and methionine and with intracellular glutathione, *Free Radical Biol. Med. 35*, 1252−1260.

48. Hawkins, C. L., and Davies, M. J. (2005) The role of aromatic amino acid oxidation, protein unfolding, and aggregation in the hypobromous acid-induced inactivation of trypsin inhibitor and lysozyme, *Chem. Res. Toxicol. 18*, 1669−1677.

49. Nightingale, Z. D., Lancha, A. H., Jr., Handelman, S. K., Dolnikowski, G. G., Busse, S. C., Dratz, E. A., Blumberg, J. B., and Handelman, G. J. (2000) Relative reactivity of lysine and other peptide-bound amino acids to oxidation by hypochlorite, *Free Radical Biol. Med. 29*, 425−433.

50. Hawkins, C. L., and Davies, M. J. (1998) Reaction of HOCl with amino acids and peptides: EPR evidence for rapid rearrangement and fragmentation reactions of nitrogen-centered radicals, *J. Chem. Soc., Perkin Trans. 2*, 1937−1945.

51. Antelo, J. M., Arce, F., and Parajo, M. (1996) Kinetic study of the decomposition of *N*-chloramines, *J. Phys. Org. Chem. 9*, 447−454.

52. Antelo, J. M., Arce, F., Franco, J., Rodriguez, P., and Varela, A. (1988) The kinetics and mechanism of the decomposition of *N*-chloroleucine, *Int. J. Chem. Kinet. 20*, 433−441.

53. Senthilmohan, R., and Kettle, A. J. (2006) Bromination and chlorination reactions of myeloperoxidase at physiological concentrations of bromide and chloride, *Arch. Biochem. Biophys. 445*, 235−244.

54. Nagy, P., and Ashby, M. T. (2007) Kinetics and mechanism of the oxidation of the glutathione dimer by hypochlorous acid and catalytic reduction of the chloroamine product by glutathione reductase, *Chem. Res. Toxicol. 20*, 79−87.

55. Nagy, P., and Ashby, M. T. (2005) Reactive sulfur species: Kinetics and mechanism of the oxidation of cystine by hypochlorous acid to give *N*,*N*′-dichlorocystine, *Chem. Res. Toxicol. 18*, 919−923.

56. Lentner, C. (1984), *Geigy Scientific Tables: Physical Chemistry, Composition of Blood, Hematology, Somatometric Data*, Vol. 3, Ciba-Geigy, Basle.